Tamoxifen exerts direct and microglia-mediated effects preventing neuroinflammatory changes in the adult mouse hippocampal neurogenic niche

Title

Tamoxifen exerts direct and microglia-mediated effects preventing neuroinflammatory changes in the adult mouse hippocampal neurogenic niche.

Authors: Isabella Crisci[a,b,c], Sara Bonzano[a,b], Zinter Nicolas[c], Eleonora Dallorto[a,b], Paolo Peretto[a,b], Wojciech Krezel*§[c], Silvia De Marchis§*[a,b].

Author's affiliations: [a]Department of Life Sciences and Systems Biology, University of Turin, Via Accademia Albertina 13, 10123, Turin, Italy; [b]NICO – Neuroscience Institute Cavalieri Ottolenghi, University of Turin, Regione Gonzole, 10, 10043 Orbassano, Turin, Italy; [c]Institut de Génétique et de Biologie Moléculaire et Cellulaire, INSERM U1258, CNRS UMR 7104, Université de Strasbourg, Illkirch, France.

§Co-last authors

***Corresponding authors:**

*Silvia De Marchis**
Dept. of Life Sciences and Systems Biology,
Via Accademia Albertina 13,
10123 Turin- Italy
Tel. +39 011670-4682
E-mail: silvia.demarchis@unito.it

*Wojciech Krezel**
Institut de Génétique et de Biologie Moléculaire et Cellulaire (IGBMC), Inserm U1258; CNRS UMR 7104; Université de Strasbourg,
1 rue L. Fries,
Illkirch 67404, France
Tel. +33 388653349
E-mail : krezel@igbmc.fr

Acknowledgments
We thank Valerie Fraulob for mouse care and Valentina La Monica for her contribution in 3D microglia reconstruction for morphological analyses. This study was funded by Università degli Studi di Torino

‘Fondo per la ricerca locale’ to SDM and PP and PRIN 2022 2022WJFN5X to SDM; Agence Nationale de la Recherche (ANR) (MicroXignal to W.K.), and the institutional LabEx ANR-10-LABX-0030-INRT grant, managed by the ANR as part of the program Investissements d’Avenir ANR-10-IDEX-0002-02 to WK.

ABSTRACT

Tamoxifen-inducible systems are widely used in research to control Cre-mediated gene deletion in genetically modified animals. Beyond Cre activation, tamoxifen also exerts off-target effects, whose consequences are still poorly addressed. Here, we investigated the impact of tamoxifen on lipopolysaccharide (LPS)-induced neuroinflammatory responses, focusing on the adult mouse dentate gyrus neurogenic niche. We demonstrated that a four-day LPS treatment led to an increase in microglia, astrocytes and radial glial cells with concomitant reduction of newborn neurons. These effects were counteracted by a two-day tamoxifen pre-treatment. Through selective microglia depletion, we elucidated that both LPS and tamoxifen influenced astrocytes and radial glial cells via microglia mediated mechanisms, while the effects on neurogenesis persisted even in a microglia-depleted environment. Overall, our data reveal that tamoxifen treatment *per se* does not alter adult neurogenesis but does modulate cellular responses to inflammatory stimuli exerting a protective role within the adult hippocampal neurogenic niche.

Keywords:

Neuroinflammation, LPS, adult neurogenesis, dentate gyrus, radial glial-like cells, astrogliogenesis, microglia.

Main Points

- Tamoxifen prevents LPS-induced changes in microglia / astroglia / RGL / newborn neuron cell numbers in the adult hippocampal DG.
- These effects involve both microglia-dependent and -independent mechanisms.

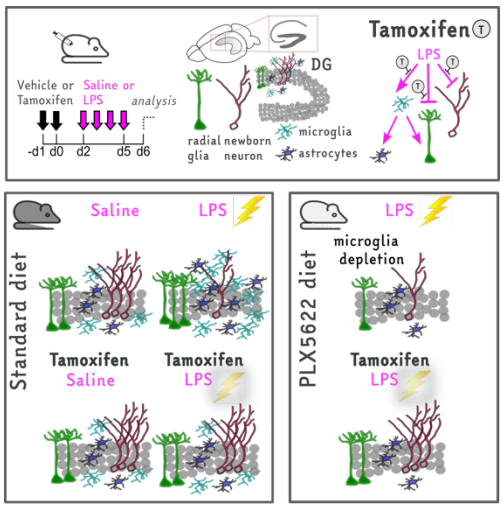

INTRODUCTION

The tamoxifen-inducible CreERT2-LoxP system has been instrumental in the last decades for the genetic labeling and manipulation of diverse cell types in the nervous system, including adult NSC/progenitor and microglial cells, to dissect the underlying cellular dynamic and molecular control (reviewed in Dhaliwal and Lagace, 2011; Imayoshi et al., 2011; Semerci and Maletic-Savatic, 2016; Dumas et al., 2021). Tamoxifen belongs to the first generation of selective estrogen receptor modulators (SERMs), initially produced in the '60s as an anti-cancer drug (Jordan, 2003), it plays either agonist or antagonist actions on estrogen receptors (ERs) in a tissue and context specific fashion (Martinkovich et al., 2014). Following administration, tamoxifen and/or its metabolites cross the blood-brain barrier reaching the brain (Lien et al., 1991; Pareto et al., 2004). In the CreERT2-LoxP genetic models, tamoxifen is administered as precursor of its more potent metabolite 4-hydroxytamoxifen (4-OHT) which binds with high affinity to the mutated form of the murine estrogen receptor ERT2 fused to Cre recombinase, allowing its translocation to the nucleus where the Cre enzyme can induce recombination of LoxP-flanked genetic sequences. Although the use of tamoxifen to induce recombination in the nervous system of CreERT2-LoxP models is widespread, only few studies have addressed its effects on the nervous tissue beyond CreERT2 activation. Interestingly, while Rotheneichner et al., (2017) reported no persisting effects on adult hippocampal neurogenesis upon tamoxifen activation of Cre-mediated recombinase, other studies have shown long-lasting adverse effects of tamoxifen on neurogenesis in both embryonic and juvenile brains (Lee et al., 2020) as well as in adult brains (Smith et al., 2022). On the other hand, tamoxifen has been reported to exert anti-inflammatory and neuroprotective therapeutic activity in different pathologies, including spinal cord injury (Colón and Miranda, 2016; Tian et al., 2009), retinal diseases (Wang et al., 2017), and aneurysmal subarachnoid

hemorrhage (Sun et al., 2013), where its neuroprotective effect was correlated with a decreased microglial activation and reduced production of inflammatory mediators. Thus, it is still controversial if and how tamoxifen treatments used to activate the Cre recombinase in animal models interfere with neurogenesis and no data are available on the consequences of such treatments on neuroinflammation. In this study, we addressed these issues specifically in the adult hippocampus, a brain region which plays a significant role in cognitive processes such as memory, learning, and mood control, and is characterized by continuous neurogenesis (Bonaguidi et al., 2012; Bond et al., 2015; Kempermann et al., 2015; Deng et al., 2010; Gonçalves et al., 2016). Indeed, the dentate gyrus (DG) in adult mice harbors a subgranular zone (SGZ) containing radial glial-like (RGL) neural stem cells (NSCs) that give rise to proliferating progenitors, which eventually produce new dentate granule neurons and astrocytes (Berg et al., 2018; Bonaguidi et al., 2011; Encinas et al., 2011; Kempermann et al., 2015; Song et al., 2012). This process is tightly regulated by cell-intrinsic elements (Bonaguidi et al., 2011; Bonzano et al., 2018; Encinas et al., 2011) and influenced by multiple environmental or physio-pathological factors that can increase (e.g., enriched environment or voluntary exercise) or decrease (e.g., aging, stress, and neurodegenerative diseases) the production and integration of adult-born neurons (Aimone et al., 2014; Beccari et al., 2017; Dranovsky et al., 2011; Gebara et al., 2016; Sierra et al., 2015; Steiner et al., 2004, 2008). Such factors can also enhance astrogliogenesis, often displaying opposite effects compared to neurogenesis. For instance, in the context of neuroinflammation, decreased neurogenesis occurs (Bonzano et al., 2018; Ekdahl et al., 2003; Fujioka and Akema, 2010; Kohman and Rhodes, 2013; Monje et al., 2003), while astroglia and microglia activation takes place (Perry et al., 2010; Pérez-Domínguez et al., 2017; Wu et al., 2012; Zonis et al., 2013). Importantly, microglial cells play key roles in the healthy DG by "surveying" the neurogenic niche to maintain homeostasis and fine-tune adult neurogenesis, being responsible for multiple functions, including phagocytosis of cellular debris and synaptic pruning (Diaz-Aparicio et al., 2020; Ekdahl, 2012; Sierra et al., 2014). Moreover, microglia neuroinflammatory responses have been associated with synaptic deficits in the CA1 hippocampal region accompanied by prolonged cognitive impairments (Jung et al., 2023). However, the potential effect of tamoxifen on microglia both in naïve conditions and in response to an inflammatory challenge and the relative effects on DG neurogenesis and astrogliogenesis remains largely unknown.

Here, we investigated the consequences of a two-day tamoxifen administration in both healthy mice and mice that received a four-day treatment with the pro-inflammatory agent lipopolysaccharide (LPS) (Cardona et al., 2006; Norden et al., 2016). Our study focused on assessing the impact of tamoxifen in the presence or absence of LPS treatment on DG microglia, astrocytes, RGL/progenitor cells, and newborn neurons through morphometric analysis. Additionally, to specifically investigate the role of microglia in mediating the effects of tamoxifen and LPS on the adult DG, we adopted a chronic treatment

with PLX5622, an inhibitor of the colony-stimulating factor 1 receptor (CSF1R), which is essential for microglia survival (Elmore et al., 2014; Green et al., 2020), and analyzed the results on the DG neurogenic niche.

METHODS

1. EXPERIMENTAL MODEL AND SUBJECT DETAILS

1.1. Ethics statement

All experimental procedures were conducted in accordance with the Guide for the Care and Use of Laboratory Animals of the European Community Council Directives (2010/63/EU and 86/609/EEC) and approved by the Italian Ministry of Health, and the French Ministry for Higher Education and Research (authorization number 864/2018-PR to SDM and 2019042614306844 to WK).

1.2. Animals

Experiments were performed on adult C57BL6 mice aged from 2 to 3 months at the onset of the experiment. Mice were housed under a 12-hour light/dark cycle as groups of three to five animals per cage in an environmentally controlled room with access to food and water *ad libitum*. Experiments were designed to minimize the number of animals used (N=65 total animals used for the study, both sexes). Mice were randomized from each group.

2. METHOD DETAILS

2.1. Drug treatments (i.e., administration of tamoxifen, LPS, PLX5622)

The following groups were used for molecular and cellular analyses of various hippocampal cell populations at shorter (forty-eight hours post injections; 48 hpi) and longer (seven days post injections, 7dpi) chase periods between two treatments. For all short-chase experiments (Figures 1-3), tamoxifen (Tam; T-5648, Sigma-Aldrich) was dissolved in corn oil (C8267, Sigma-Aldrich) and used as a pretreatment by daily intraperitoneal (i.p.) injections of 2.5 mg/mouse/day, for two consecutive days. Tamoxifen administration was then followed, after 48 hours, by daily i.p. injections of either *E. coli*-derived lipopolysaccharide (LPS; 0.5 mg/kg/day) for four consecutive days (L2880, Sigma-Aldrich) in the *Tam+LPS* group or saline physiological solution as a control (Sal; 0.9%) in the *Tam+Sal* group. The other two groups, named Sal or LPS solely, were injected with Tam vehicle (i.e., corn oil) followed by either saline or LPS, respectively. For the analysis of the effect of tamoxifen pretreatment on neuroinflammation elicited at a longer chase period (Figure 4), mice named *L-Tam+LPS* were injected with LPS (0.5 mg/kg/day) seven days after tamoxifen injections (7dpi), once a day for four consecutive days, and compared to the mice that received only LPS (i.e., *LPS* group). All experimental groups were then sacrificed one day after the last LPS or Sal injection for analyses. A sample size of at least three

mice was randomly assigned to each experimental group, and the number of animals used for each experiment is specified in figure legends.

Pharmacologic ablation of brain microglia was obtained by administration of the CSF1R inhibitor PLX5622 (Plexxikon, Inc.; Berkley, CA) formulated at 1200 parts per million (ppm) into standard rodent diet AIN-76A (12% fat, caloric density 3.86kcal/g; Research Diets, Inc. (New Brunswick, NJ). Animals were fed *ad libitum* with either the PLX5622 formulated diet or a standard chow diet (AIN-76A) starting from five days before receiving the first Tam/corn oil injection and for the entire duration of the experiment.

2.2. Tissue preparation and sectioning

For immunofluorescence analysis, mice were deeply anesthetized with a mixture of tiletamine/zolazepam (80 mg/kg, Zoletil 100, Virbac Corporation, France) by i.p. injection, and perfused transcardially with ice-cold 0.9% saline solution, followed by ice-cold 4% paraformaldehyde (PFA, Sigma-Aldrich 441244) in 0.1 M phosphate buffer (PB), pH 7.4. Brains were removed from the skull and postfixed for 4 hours in the same PFA solution at 4°C. Post-fixation was followed by a cryopreservation step with a 30% sucrose solution in 0.1 M PB pH 7.4 at 4 °C for 48 hours. Then, the two hemispheres were separated and embedded in optimal cutting temperature compound (OCT, Killik, Bio-Optica), frozen, and stored at −80 °C until sectioning. One hemisphere was then cut with a cryostat (Leica Microsystems), and serial free-floating 30µm-thick coronal sections were collected in multi-well dishes and stored at −20°C in antifreeze solution (30% ethylene glycol, 30% glycerol, 10% PB: 189 mM NaH2PO4, 192.5 mM NaOH; pH 7.4) until use.

2.3. Multiple immunofluorescence labeling

Brain sections were rinsed in phosphate buffer solution (PBS, 0.01M, pH 7.4) and pre-incubated at room temperature (RT) for 1 h in PBS containing 10% of the normal sera that matched the host species of the secondary antibodies (i.e., normal donkey serum, NDS; Jackson ImmunoResearch, 017-000-121) and 0.5% Triton X-100 (Sigma-Aldrich T8787) for blocking unspecific bindings. Then slices were incubated with primary antibodies (for dilution see Table S8a) diluted in PBS containing 0.5% Triton X-100 and 1% NDS at 4°C for 48 hours. After three rinses in PBS, slices were incubated with the appropriated fluorochrome-conjugated secondary antibodies (for dilutions Table S8b) in PBS for 1,5 h at RT. Sections were finally counterstained with the nuclear dye 4′,6-diamidino-2-phenylindole (DAPI; 1:1000; Sigma-Aldrich, D9542) for 15 minutes at RT and coverslipped with the anti-fade mounting medium Mowiol (4-88 reagent, MIllipore 475904).

2.4. Confocal microscopy

Confocal images were acquired with a TCS SP5 confocal microscope (Leica Microsystems). Images were captured as z-stacked focal planes through the thickness of the slice (30 µm) at 1-µm optical steps with an oil-immersed Plan-Apochromat 40X/1.25 objective, zoom 1.0, and resolution of 1024/1024 pixels and 100Hz (1 pixel = 0.38 µm) comprising both upper and lower blades of the hippocampal DG.

2.5. Cell counting and morphometric analyses

For cell quantification, images were analyzed with NIH ImageJ (https://imagej.nih.gov/ij/) using the cell counter and channel tool plugins. At least three different levels along the rostrocaudal DG axis were analyzed, and the cell density was calculated by dividing the total number of counted cells over the area of interest (MCL, SGZ+GCL, or Hilus) and expressed as the mean number of cells per squared millimeters (cells/mm^2). Microglia cells were visualized by Iba1 expression and counted separately in each DG region (MCL, SGZ/GCL, and Hilus). For DCX and NeuroD1 analysis, immunopositive cells were counted in the SGZ and deep GCL area, where DAPI staining was used to trace the granule cell layer in DG and counterstain clustered cells discriminating single marker+ cells among packaged marker+ cells. For analysis of GFAP+ RGL, cells were deemed radial if the cell body, clearly associated with a DAPI+ nucleus, was located in the SGZ and had a single thin radial process extending throughout GCL and branching into the MCL (Gebara et al., 2016).

For microglia morphological analyses, tridimensional reconstruction of Iba1+ cells was performed in z-multi-stack with NIH ImageJ using Simple Neurite Tracer (SNT) plugin upon manual image editing (i.e., subtract background and grayscale attribute filtering). Then, manual 3D reconstruction was finalized with the filling tool to measure morphological parameters: the territory area as the convex hull area, where the convex hull is the smallest convex polygon (that with all interior angles smaller than 180◦) containing the whole-cell shape (Fernández-Arjona et al., 2017), and to carry out 2D Sholl-analysis by exploiting the Sholl plugin.

2.6. Tissue collection, RNA extraction, and RT-qPCR

For whole-hippocampus RT-qPCR, mice were sacrificed by cervical dislocation, and hippocampi were microdissected and quickly frozen in liquid nitrogen and stored at − 80 °C until further processing. Total RNA was extracted from brain homogenate using RNeasy Micro Kit (Qiagen, France) following the manufacturer's protocol. Reverse transcription was carried out using the QuantiTect kit (Qiagen, France). The qPCR reactions were performed in duplicates in a LightCycler480 (Roche) using QuantiTect SYBR Green PCR kit (Qiagen, France) and gene-specific primers (Key Resources Table). The number of transcripts was evaluated relative to the expression level of the housekeeping gene acidic ribosomal phosphoprotein P0 (Rplp0 or 36B4). Fold change was calculated with respect to the control saline-injected group.

3. QUANTIFICATION AND STATISTICAL ANALYSIS

Results were presented as mean ± s.d. and derived from at least three different animals/group. A two-tailed independent t-test was performed to compare the differences between two groups; moreover, an F-test of equality of variances was conducted to compare variances, and Welch's correction was applied in case of unequal variance distribution. Kruskal-Wallis test and Dunn's multiple comparison test were used for statistical analysis for qPCR analyses to compare fold change in mRNA expression to the saline-control mean. Then, for cellular analyses, Two way analysis of variance (ANOVA) with Student-Newman-Keuls' post hoc test was used for multiple comparisons of unequal sample sizes regardless of rows and columns. Data distribution was assumed to be normal with the Shapiro-Wilk test (alpha=0.05). The confidence interval was expressed with 95% confidence. The statistical significance was defined as follows: *p<0.05, **p<0.01, and ***p<0.001. All statistical analyses were performed using Microsoft Excel and Graphpad Prism 8 software. For cell counting, outliers were identified with Tukey's method following 1.5xIQR (Interquartile range) rule.

4. DATA AVAILABILITY

All data reported in this paper will be shared by the corresponding authors upon request.
Any additional information required to reanalyze the data reported in this paper is available from the lead contact upon request.

KEY RESOURCES TABLE

REAGENT or RESOURCE	SOURCE	IDENTIFIER
Antibodies		
Rabbit polyclonal anti-Iba1 (1:1000)	FUJIFILM Wako Shibayagi	Cat# 019-19741; RRID:AB_839504
Goat polyclonal anti-DCX (1:1500)	Santa Cruz Biotechnology	Cat# sc-8066; RRID:AB_2088494
Goat polyclonal anti-NEUROD1 (1:400)	Santa Cruz Biotechnology	Cat# sc-1084; RRID:AB_630922
Goat polyclonal anti-GFAP (1:200)	Abcam	Cat# ab53554; RRID:AB_880202
Mouse monoclonal anti-GFAP (1:700)	Immunological Sciences	Cat# MAB-12029;
Rabbit anti-S100 beta (1:10000)	Swant	Cat# 37A; RRID:AB_2315305
Rabbit polyclonal anti-Ki67 (1:1000)	Abcam	Cat# ab15580; RRID:AB_443209
Alexa Fluor 488 donkey anti-Mouse (1:400)	Jackson ImmunoResearch Labs	Cat# 715-545-151; RRID:AB_2341099
Alexa Fluor 488-AffiniPure Donkey Anti-Rabbit IgG (H+L) (1:400)	Jackson ImmunoResearch Labs	Cat# 711-545-152; RRID:AB_2313584
Alexa Fluor 647 AffiniPure F(ab')$_2$ Fragment Donkey Anti-Rabbit IgG (H+L) (1:600)	Jackson ImmunoResearch Labs	Cat# 711-606-152; RRID:AB_2340625

Cy™3 AffiniPure Donkey Anti-Goat IgG (H+L) (1:800)	Jackson ImmunoResearch Labs	Cat# 705-165-147; RRID:AB_2307351
Chemicals, peptides, and recombinant proteins		
Lipopolysaccharide (LPS) (E.coli (O55:B5)	Sigma-Aldrich	L2880
PLX-5622	Plexxikon, Inc.; Berkley, CA	PLX-5622
Tamoxifen	Sigma-Aldrich	T5648
corn oil	Sigma-Aldrich	C8267
Killik OCT	Bio-Optica	05-9801
DAPI	Sigma Aldrich	D9542
Zoletil	Virbac	N/A
Paraformaldehyde	Sigma-Aldrich	441244
Mowiol 4-88 reagent	Millipore	475904
Triton X-100	Sigma-Aldrich	T8787
Critical commercial assays		
QuantiTect SYBR Green PCR kit	Qiagen	204145
Experimental models: Organisms/strains		
Mouse: C57BL/6J	JAX	632
Mouse: C57BL/6N	Charles River	6NCrl
Oligonucleotides-Primers for qPCR reactions		
TNFα -F (5-CTTCTGTCTACTGAACTTCGGG-3)	Sigma-Aldrich	TNFα -F
TNFα -R (5-CAGGCTTGTCACTCGAATTTTG-3)	Sigma-Aldrich	TNFα -R
IL1β-F (5-ACGGACCCCAAAAGATGAAG-3)	Sigma-Aldrich	IL1β-F
IL1β-R (5-TTCTCCACAGCCACAATGAG-3)	Sigma-Aldrich	IL1β-R
IL6-F (5-CAAAGCCAGAGTCCTTCAGAG-3)	Sigma-Aldrich	IL6-F
IL6-R (5-GTCCTTAGCCACTCCTTCTG-3)	Sigma-Aldrich	IL6-R
IL4R-F (5-ATTGTCTACTCAGCCCTTAC-3)	Sigma-Aldrich	IL4R-F
IL4R-R (5-CAGCAGCCACAGCAAGGACT-3)	Sigma-Aldrich	IL4R-R
TGFb-F (5-TGATACGCCTGAGTGGCTGTCT-3)	Sigma-Aldrich	TGFb-F
TGFb-R (5-CACAAGAGCAGTGAGCGCTGAA-3)	Sigma-Aldrich	TGFb-R
Rplp0 (36B4) (5-ACCCTGAAGTGCTCGACATC-3)	Sigma-Aldrich	Rplp0
Rplp0 (36B4) (5-AGGAAGGCCTTGACCTTTTC-3)	Sigma-Aldrich	Rplp0
Software and algorithms		
Graphpad Prism 8 software	GraphPad Software	https://www.graphpad.com/scientific-software/prism/
ImageJ	Schneider et al., 2012	https://imagej.nih.gov/ij/
Other		
Confocal microscope	Leica Microsystems	TCS SP5
Cryostat	Leica Microsystems	CM1860
LightCycler480	Roche	05015278001

RESULTS

Tamoxifen impacts hippocampal DG microglia and prevents its expansion upon LPS treatment

Tamoxifen can exert either detrimental or neuroprotective actions including anti-inflammatory activity on the nervous tissue in various experimental or clinical conditions (Lee et al., 2020; Smith et al., 2022; Baez-Jurado et al., 2019). Here, we investigated whether a short tamoxifen treatment, as used for inducible DNA recombination based on the CreERT2-LoxP system (Bonzano et al., 2018; Rolando et al., 2012; Yang et al., 2015; Nato et al., 2015; Bonzano et al., 2023), interferes with the response of nervous tissue to a repeated peripheral inflammatory stimulus and how this impacts adult hippocampal neurogenesis.

We treated adult mice with tamoxifen (2.5mg/mouse/day) or its vehicle (i.e., corn-oil) once a day over two consecutive days, followed by an intraperitoneal (i.p.) injection of *E. coli*-derived lipopolysaccharide (LPS, at a dose of 0.5 mg/kg/day) or saline solution (Sal, as control), 48 hours later and repeated for four days to mimic chronic inflammation (***Fig. S1A***). We initially focused our analysis on microglial cells, which sense and contribute to neuroinflammatory signaling by the early release of cytokines associated with an increased number and modified morphology (Chen et al., 2012; Morganti et al., 2016; Norden et al., 2016; Walker et al., 2014), and which control the microenvironment of the adult neurogenic niche (Diaz-Aparicio et al., 2020; Ekdahl, 2012; Gebara et al., 2013; Sierra et al., 2010; Zhang et al., 2020).

The brain tissue was processed for immunofluorescence staining for the cytoplasmic microglia marker Iba1 (Ito et al., 1998), followed by confocal laser scanning microscopy coupled to morphometric analyses (***Fig. 1***). We first assessed the cell density of Iba1+ microglia within the whole DG and found an increase in LPS-injected mice compared to control mice (Sal). Interestingly, this effect was prevented by tamoxifen pre-treatment in Tam+LPS mice, while tamoxifen alone (i.e., Tam+Sal) did not alter microglial cell density (***Fig. 1A,B***). A similar trend was observed by analyzing separately the different DG layers (i.e. granule cell layer-GCL; molecular cell layer MCL and hilus) with statistically significant effects obtained for the GCL (Sal vs LPS and LPS vs Tam+LPS) and MCL (Sal vs LPS) (***Fig S1B***).

While the LPS-treated group exhibited an increase in microglial cell density compared to the control group, this did not correspond to a proportional expansion of the area covered by the Iba1+ microglia (i.e., microglia fractional area; ***Fig. 2C and Fig. S1C***). To disclose possible alterations in microglia morphology at a single cellular resolution, we employed three-dimensional reconstructions of individual Iba1+ cells (***Fig. 1D***) (Davis et al., 2017). Analysis of the territory area, calculated as the smallest convex polygon encompassing the whole microglia cell shape (Fernández-Arjona et al., 2017), revealed a

reduction in the group treated with LPS compared to the saline group (***Fig. 1E***). This reduction was associated with a decrease in the complexity of microglial processes in LPS-treated mice when compared to controls (***Fig. 1F,G***). The pre-treatment with tamoxifen did not prevent these changes in LPS-treated mice (***Fig. 1E-G***). In addition, mice that received only tamoxifen also displayed a net reduction in microglia fractional area (***Fig. 1C***), both in comparison to saline and LPS-treated groups, suggesting that tamoxifen alters microglia morphology independently of LPS-induced effects. Accordingly, Sholl analysis revealed an impact of tamoxifen on the spatial distribution of microglial ramification in the TAM+Sal group. This resulted in an intermediate morphotype between the LPS and Sal groups characterized by a significant reduction in ramifications compared to the saline group at radial distances proximal to the soma (i.e., 16 to 24 micrometers from the soma) (***Fig. 1F***). Analysis of the soma size of microglial cells revealed no differences among the different groups (***Fig. S1D***). This suggest that morphological changes induced by either LPS or tamoxifen primarily affect microglial processes.

In parallel to the morphological analyses, we conducted RT-qPCR analyses on hippocampal tissue extracts to quantify the gene expression of selected inflammatory molecules (***Fig. 2***, ***Tab. S2***). We found a 6 fold increase in the expression of the pro-inflammatory mediator IL-1β in LPS-treated mice that was not prevented by tamoxifen pre-treatment (***Fig. 2A***). While no statistically significant differences were observed for TNFα (***Fig. 2B***), tamoxifen led to a moderate up-regulation of IL-6 (both in absence and presence of LPS ***Fig. 2C***) IL-4R (in absence of LPS ***Fig. 2D***) and TGFβ (in presence of LPS, ***Fig. 2E***).

Overall, these data indicate that a two-day-long tamoxifen treatment impacts microglia morphology and can modulate the expression of pro- and anti-inflammatory mediators in the hippocampus. Notably, this treatment prevents an increase in microglia cell numbers caused by a four day-long LPS treatment, but does not reverse the changes in microglia morphology or selected inflammatory signals associated with the LPS treatment.

Tamoxifen prevents the LPS-induced dysregulation in astroglia, RGL cells and newborn neurons of the adult DG

Alongside microglial cells, astrocytes are actively involved in the brain tissue response to inflammatory challenges (Lana et al., 2017; Norden et al., 2016; Yang and Zhou, 2019). To assess the possible effects of tamoxifen on the astroglial population within the DG neurogenic niche, we quantified glial fibrillary acidic protein-positive (GFAP+) astrocytes in the GCL and subgranular zone (SGZ) (***Fig. 3A,B***). The density of GFAP+ astrocytes was increased in LPS mice compared to Sal control mice, and tamoxifen prevented such an increase in Tam+LPS mice (***Fig. 3B***). We further analyzed S100β immunostaining, a marker of astrocyte maturation whose upregulation is associated with reactive astrocytes (Reid and

Kuipers, 2021). On average, nearly 70% of GFAP+ astrocytes were double-positive for S100β (*magenta bars in* ***Fig. 3B***) and both S100β -positive and S100β-negative GFAP+ cells followed the same global dynamics in the different treatments as the total GFAP+ astrocytes (***Fig. 3A,B***). GFAP is also expressed by RGL cells whose cell body is located in the SGZ (***Fig. 3A,C***). Quantification of GFAP+ RGL cells in LPS-treated mice revealed an increase in their number, which was prevented by tamoxifen in the Tam+LPS groups (***Fig. 3C***). A similar trend was observed for double labeled S100β+GFAP+ RGL cells, which represent a subset of non-proliferating RGL (i.e., type β RGL) in a transition phase towards astrocyte differentiation (Gebara et al., 2016) (*magenta bars in* ***Fig. 3C***). Overall, these data indicate that RGL cells and DG astrocytes respond similarly to LPS and tamoxifen treatments.

We next used Doublecortin (DCX) as a marker for neurogenesis -labeling type2 progenitors, neuroblasts and immature neurons (Steiner et al., 2006)- to further investigate the impact of tamoxifen treatment on the DG (***Fig. 3D,E***). Notably, we found no differences in DCX+ cell density between Sal and Tam+Sal groups (***Fig. 3E***), indicating that tamoxifen alone did not cause significant changes in the density of DCX+ cells. In contrast, a reduction in DCX+ cells was observed in the LPS group compared to the Sal group (***Fig. 3D,E***) and this effect was prevented by tamoxifen pre-treatment in Tam+LPS mice (***Fig. 3E***). A protective effect on DG neurogenesis upon tamoxifen treatment in LPS injected mice was further confirmed by analysis of NeuroD1, a bHLH transcription factor whose expression largely overlaps with DCX and whose function has been associated to survival and maturation of adult-born neurons (Gao et al., 2009) (***Fig. 3F,H and Fig. S2E, F***).

Quantification of the proliferation marker Ki67 in the DG of the different groups revealed no changes in the density of the whole Ki67+ cell population (***Fig.S2A-B***). Moreover, we also evaluated the density of GFAP+/Ki67+ RGL cells (i.e., active RGL; ***Fig.S2C-D***) and SGZ type 2 progenitors, discriminating between type 2a progenitors (i.e., GFAP-/NeuroD1-/Ki67+;***Fig. S2G***) and type 2b progenitors and neuroblasts (NeuroD1+/Ki67+; ***Fig. 3G***). We did not find differences among groups (***Fig. S2D and G*** *and* ***Fig. 3F,G***), indicating that at the time point of the analysis (i.e., 24 hr after the last LPS injection) the different subpopulations of proliferating SGZ cells were not affected by LPS and/or tamoxifen treatments. Conversely, the number of postmitotic immature neurons (i.e., NeuroD1+/Ki67- cells), was reduced in LPS group, while in Tam+LPS mice it was comparable to controls (i.e. Sal group; ***Fig. 3F,H***), pointing to a protective pro-survival role of tamoxifen on adult-born neurons.

Overall, these findings show that while in control conditions a two-day tamoxifen treatment does not alter the balance among the main cell populations in the adult DG neurogenic niche, it consistently counteracts the LPS-induced dysregulation normalizing numbers of astrocytes, RGL cells and newborn neurons.

Long-term preventing effect of tamoxifen against LPS induced changes

According to pharmacokinetic studies in mice, tamoxifen and its active metabolites are completely degraded to negligible levels in the brain within 7 days (Jahn et al., 2018; Valny et al., 2016). We thus ran an additional experiment performing tamoxifen pre-treatment (single i.p. injection for two consecutive days) one week before the start of a four-day-long LPS treatment (i.e., Long-chase; L-Tam+LPS). Interestingly enough, quantification of Iba1+ microglia on L-Tam+LPS treated mice revealed a reduction in microglia cell density and in the fractional area of Iba+ staining compared to LPS group (***Fig. 4A,B***). Although this long-term effect of tamoxifen was attenuated compared to the one observed in the short-term protocol (***Fig. 1***), these data suggests that the consequences of tamoxifen treatment may exceed its bioavailability period. Accordingly, a tendency to a reduced number of GFAP+ astrocytes was found in L-Tam+LPS versus LPS mice (P= 0.0569; ***Fig. 4D***) and quantification of GFAP+ RGL cells and DCX+ newborn neurons confirmed a long-term preventing effect of tamoxifen against LPS induced changes on these cell populations (***Fig. 4E,F***).

The effects of tamoxifen and LPS on the adult DG imply both microglia-dependent and microglia-independent mechanisms

Our data clearly indicate that tamoxifen and LPS treatments impact multiple cellular components of the dentate gyrus SGZ and GCL. However, the interdependence of the observed changes remains unclear. To get a deeper insight into the role of microglia in this context, we exploited a pharmacological strategy by oral administration (diet supplement) of Plexxikon (PLX)5622 to deplete microglia in the CNS (Elmore et al., 2014; Green et al., 2020). The effectiveness of the PLX5622 treatment was confirmed by a drastic reduction in Iba1+ microglia in the DG of mice that received a 5-day treatment as compared to standard chow-diet fed mice (***Fig. S3A, B***). Therefore, we designed an experimental protocol including PLX5622 administration, which started 5-days before tamoxifen or vehicle administration, followed by saline or LPS injections 2 days later (***Fig. S3C***). Mice were maintained under continuous PLX5622 treatment throughout the whole experiment (i.e., from -d6 to d6 for a total of 12 days) to avoid the repopulation of microglia (Huang et al., 2018). The day after the last saline or LPS injection, only rare Iba1-immunopositive cells were observed in the DG of PLX5622 treated mice (***Fig. 5A)***. Notably, in those mice, LPS treatment did not result in an increase in the number of microglial cells in the GCL and Hilus (***Fig. 5C,D***). Although in the MCL the residual microglial cells were still responsive to LPS (***Fig. 5B)***, their number corresponded roughly to 10% of that quantified in control condition. Overall, the reduction in the DG ranged from 86% to 97% (***Fig. 5B-D***), proving the efficacy of PLX5622 treatment.

Quantification of DCX+ cells in the DG of microglia-depleted mice revealed a decrease in LPS group compared to Sal group, which was prevented by tamoxifen pre-treatment in PLX+Tam+LPS group (***Fig. 5E, F***). A similar effect was observed also for GFAP+ RGL cells (***Fig. 5G,H***), with a LPS-induced reduction in number that was prevented by tamoxifen. Intriguingly, while the effect of LPS on DCX+ cells in microglia-depleted mice is in line with those found in presence of microglia, the effect of LPS treatment on RGL cells exhibits an opposite trend, with an increase observed in the presence and a decrease in the absence of microglia. Finally, no differences were found in the number of GFAP+ astrocytes among the different groups (***Fig. 5G,I***). These findings indicate that microglial cells are needed to elicit the LPS-induced changes observed in the astrocytic population and are involved in the modulation of the RGL cell population, but they are dispensable for the effects produced by LPS on DG neurogenesis. Overall, our data demonstrate that tamoxifen prevents direct and microglia-mediated LPS-induced changes in the adult hippocampal neurogenic niche.

DISCUSSION

Tamoxifen is a widely approved treatment in breast cancer therapy in humans, but its off-label use is also frequent in several clinical conditions (Farrar and Jacob, 2023). Its prescription needs to be highly patient-specific as it may act both as ER antagonist (e.g. to exert cytostatic effects in breast) or agonist (e.g. promoting bone density) in a cell and tissue-dependent manner. Thus, better understanding of the mechanisms of tamoxifen actions is critical for successful treatments. Similarly, knowledge of biological tamoxifen effects is essential for interpretation of studies employing the tamoxifen-inducible CreERT2/LoxP system as a highly effective and widely used genetic tool for manipulating gene expression in specific cell types in a temporally controlled manner (Whitfield et al., 2015).

A two-day tamoxifen administration in adult mice does not alter DG neurogenesis

In this study, we addressed tamoxifen effects on the adult DG neurogenic niche using a two-day tamoxifen administration at the dose of 2.5 mg/mouse/day, which roughly corresponds to an average of 100 mg/kg/day, in adult wild-type mice aged 8-12 weeks. This protocol has been previously used to achieve efficient DNA recombination in adult NSCs using the CreERT2-LoxP system (Bonzano et al., 2018; Rolando et al., 2012; Yang et al., 2015; Nato et al., 2015; Bonzano et al., 2023). Our data revealed that tamoxifen treatment alone did not affect the cellular composition of the adult DG, leaving unaltered the density of radial-glia NSCs and proliferating progenitors, as well as the number of newborn immature neurons within the SGZ/GCL of adult mice. These findings are in line with a previous report (Rotheneichner et al., 2017) documenting absence of changes in DG progenitor proliferation and newborn neuron generation/survival following administration of 100 mg/kg/day tamoxifen for five days. Similarly, a recent study employing a tamoxifen administration scheme of 180mg/kg/day for five days

showed no consequences on the DCX+ newborn neuron generation/survival, while highlighting a suppression of intermediate progenitor cell proliferation at three weeks after treatment, suggesting long-term effects (Smith et al., 2022). Long-term detrimental effects of tamoxifen administration on adult neurogenesis have been also reported in embryonic and adolescent mouse brains (Lee et al., 2020). In particular, this latter study revealed that a 2mg/animal dose per day (corresponding roughly to 170 mg/kg/day for an average weight of 12gr at 3-4 weeks of age) lasting five days, reduced proliferating cells in the postnatal DG and subventricular zone (SVZ; i.e. the other neurogenic niche in the adult brain). Two major differences in experimental design are likely to explain the discrepancy in findings when comparing these and our data: i) the total amount of tamoxifen administered (i.e. higher in Lee and Smith studies compared to Rotheneichner and our current study), and ii) the age of treated animals, which were younger in Lee's study. Specifically, the postnatal animals tested in Lee's study were around puberty, a critical stage of life characterized by sex steroid-dependent brain structural organizational changes (Siks et al., 2005), involving significant shaping of adult neurogenesis in rodents (Oboti et a., 2017; Trova et al., 2020 and 2021). Thus, because tamoxifen can exert both agonistic and antagonistic estrogenic effects, the peripubertal neurogenic niches could be particularly susceptible to tamoxifen. Finally, age differences might be relevant considering recent reports indicating a change in the dynamics and behaviors of DG NSCs between juvenile and adult life (Harris et al., 2021; Ibrayeva et al., 2021), which could imply different vulnerability to tamoxifen.

Tamoxifen interferes with LPS-driven neuroinflammatory response in the adult mouse hippocampal neurogenic niche

The systemic administration of LPS is a reliable method to elicit a rapid innate immune response in the brain, whose effects at the cellular and molecular levels vary according to the experimental protocol (Batista et al., 2019; Norden et al., 2016). Here, we exploited a protocol based on injecting mice with a low dose of LPS (0.5 mg/kg) for four consecutive days. This protocol led to a moderate increase of the pro-inflammatory cytokine IL-1β in the hippocampi of LPS-treated mice, as measured at 24hrs after the last LPS treatment. These data are consistent with previous studies showing that repeated LPS challenge elicits an attenuated inflammatory molecular profile in the brain than the response observed following an acute single-dose LPS challenge, indicating immune tolerance (Norden et al., 2016, Wendeln et al., 2018). Yet, the data on microglial cells in the hippocampal DG support clear modifications in response to LPS treatment, both in terms of increased number and morphological changes (Fernández-Arjona et al., 2017; Madore et al., 2013; Norden et al., 2016; Stence et al., 2001). Importantly, these effects on microglia were associated with an increase of RGL NSCs and astrocytes and a concomitant decrease in DCX+ newborn neurons. While changes in newborn neurons and

astrocytes following LPS are well documented (Bonzano et al., 2018; Chesnokova et al., 2016; Ekdahl et al., 2003; Fujioka and Akema, 2010; Melo-Salas et al., 2018; Monje et al., 2003; Perez-Dominguez et al., 2019; Valero et al., 2014; Zonis et al., 2013), to the best of our knowledge, the observed increase in RGL NSCs following LPS injection has not been reported before. Thus, an increased astrogliogenesis could directly result from LPS-induced rise in NSCs and their increased differentiation towards astrocytes. Instead, the observed decrease in DCX+ newborn neurons following LPS could derive from the altered production or proliferation of intermediate progenitors and/or defective survival of newborn neurons. In support of this possibility the number of NeuroD1+ progenitors was reduced at the issue of LPS treatment. Furthermore, a reduction in NeuroD1+ postmitotic cells upon LPS treatment point to potential impairment in cell survival of newborn neurons that may contribute to reduced neurogenesis. Although we did not find changes in proliferating cells in the DG at 24hrs after the last LPS injection, we cannot exclude that proliferation of NSCs and/or intermediate progenitors was altered at earlier steps during LPS-treatment. Accordingly, a previous study described a detrimental effect of inflammation after a single LPS injection on cell cycle progression of type 2 intermediate progenitors, which may contribute to the decrease in the birth rate of DG neurons (Melo-Salas et al., 2018).

Notably, a two-day tamoxifen treatment was able to prevent the increase in microglia numbers as well as the decrease of immature neurons and the parallel increase in DG astrocytes and RGL cells induced by LPS injections. Moreover, tamoxifen alone was sufficient to alter the morphology of microglial cells in the DG and to moderately increase the expression of inflammatory mediators within the adult mouse hippocampus. These findings support the role of tamoxifen in regulating microglia state and their responsiveness to inflammatory stimuli, possibly contributing to immune tolerance. Understanding the exact molecular mechanisms underlying the tamoxifen-dependent prevention of the detrimental effects in response to LPS deserves further investigation, but our data suggest that they are not mediated by a pure regulatory role at the level of gene expression, at least with respect to cytokines analyzed in present study. Indeed, an increased expression of pro-inflammatory cytokines at 24hrs after ceasing LPS administration was observed even in tamoxifen pretreated mice as reflected by augmented expression of IL-1β and IL-6, which were concomitant with an increase of the IL-4R and TGFβ expression, classically known to contribute to anti-inflammatory signaling. Microglia trophic support known to play a role in the control of proliferation, survival and differentiation of neural progenitors (Frost and Schafer, 2016) may also be involved in microglia-dependent beneficial effects of tamoxifen on the DG neurogenic niche.

Microglia mediate LPS and tamoxifen effects on adult RGL cells and astrocytes but not on newborn neurons in the murine DG

To further investigate the involvement of microglia in LPS- and tamoxifen-driven effects on the DG, we treated mice with PLX5622 to deplete microglia in the CNS (Elmore et al., 2014; Green et al., 2020). We found that the increased number of astrocytes and RGL observed in LPS-treated mice was critically dependent on the activity of microglia, as such effects were lost in microglia-depleted mice. In fact, in absence of microglia, LPS treatment significantly reduced the number of RGL NSCs, exerting an opposite effect to that observed without microglia depletion. Therefore, we propose that the outcome of LPS treatment on RGL cells is mediated through two competing mechanisms, an indirect microglia-dependent stimulating activity that dominates and masks a negative regulation on RGL cell numbers, possibly mediated through cell-autonomous mechanisms.

Tamoxifen effects are mechanistically mediated by activation of the nuclear ERs and/or the membrane-bound G-protein-associated estrogen receptor (GPR30) (Arevalo et al., 2015; Baez-Jurado et al., 2019). The expression of both receptors by microglia and astrocytes have been documented and reported to be involved in inflammatory responses, a powerful regulator of adult hippocampal neurogenesis (Arevalo et al., 2012; Correa et al., 2019; Garcia-Ovejero et al., 2005; Leiter et al., 2016; Sierra et al., 2008; Vicidomini et al., 2020). Accordingly, these receptors could be involved in indirect, microglia-dependent effects of tamoxifen on astrogliogenesis. Thus, whereas the lack of an increase in astrocyte number after LPS treatment in microglia-depleted mice supports a key role of microglia in LPS-induced astrogliogenesis, the prevention of LPS-induced astrogliogenesis by tamoxifen, in presence of microglia, points that microglia are also critical mediator of such effect of tamoxifen. However, ERs and GPR30 are also expressed by adult DG NSC/progenitor cells, as well as by DG immature and mature granule neurons (Brailoiu et al., 2007; Hajszan et al., 2007; Isgor and Watson, 2005; Mazzucco et al., 2006), indicating that tamoxifen may directly regulate the response of these cells to LPS-induced effects. Accordingly, in the absence of microglia, tamoxifen prevented the LPS-induced reduction of both RGL NSCs and DCX+ newborn neurons. Thus, our data suggest the co-existence of both mechanisms of action (i.e. cell-autonomous and microglia-mediated) by tamoxifen and their differential contribution in controlling the neuron/astroglia balance in the adult DG upon neuroinflammation. We propose that interplay of these two mechanisms underlays beneficial effects of tamoxifen in LPS treated mice including microglia-mediated prevention of RGL NSC expansion and astrogliogenesis as well as direct neuroprotective action on NSCs and newborn neurons.

CONCLUSION

Overall, our findings highlight the importance of recognizing the potential immunomodulatory role of tamoxifen when used in conjunction with CreERT2-loxP transgenic mice, not only in LPS-induced neuroinflammation but also in other pathological models, including models of the experimental

autoimmune encephalomyelitis (EAE) and the toxin-mediated models of demyelination, as well as in various models of neurodegenerative diseases associated with neuroinflammation. Finally, such observations should guide future clinical investigations of pathological conditions involving inflammation and innate immune response including for example neurological diseases and cancer.

AUTHOR CONTRIBUTIONS

Conceptualization SDM, WK, IC, SB, PP; Validation SDM, SB; Formal analysis IC, SB; Investigation IC, ED, NZ; Writing – Original Draft IC, SDM; Writing – Review & Editing SDM, WK, SB, PP; Resources: SDM, WK, PP; Visualization IC, SB; Supervision: SDM; WK; Project Administration SDM, WK; Funding acquisition SDM, WK.

DECLARATION OF INTERESTS

The authors declare no competing or financial interests

MAIN FIGURE TITLES AND LEGENDS

Figure 1. Tamoxifen alters hippocampal DG microglia activation upon LPS treatment. (A) Representative confocal images showing microglia immunopositive for Iba1 (yellow) in the DG (See experimental design in Fig.S1A). Cell nuclei are counterstained with DAPI (blue). Insets show high-magnification images of Iba1+ microglial cells (arrows) for each DG subregion (MCL, molecular layer; GCL, granule cell layer; Hilus). (B) Quantification of Iba1+ microglial cell density within the DG. (C) Percentage of the area covered by Iba1+ microglial cells within the DG. (D) Examples of binarized max projections of 3D-reconstructed Iba1+ microglial cells within the DG. (E) Quantification of the territory area occupied by single microglial cells; each dot represents a cell. (F,G) Sholl analysis of microglial processes showing the distribution of ramifications (F) and the overall complexity calculated as the total number of intersections per microglial cell (G) of 3D-reconstructed microglial cells within the DG. n=3-5 mice/group (B, C). n=15-18 cell/group out of 3 mice/group (E, F, G). Scale bars, 50 µm (A; low magnification), 10 µm (A, and D; high magnification). Data are presented as mean ± SD (B, C), mean ± SEM (F) and box-and-whisker plot indicating a minimum-maximum range (E, G). Two-way ANOVA followed by a Student-Newman-Keuls (SNK) multiple comparison test: *p< 0.05, **p<0.01, ***p<0.001. Statistical values are reported in Tables S1, S1.1.

Figure 2. Tamoxifen modulates the expression of inflammatory mediators within the adult mouse hippocampus. (A-E) Fold changes in IL1β (A), TNFα (B), IL-6 (C), IL-4R (D), and TGFβ (E) gene transcripts in the hippocampi of mice injected with LPS alone (LPS) or treated with tamoxifen before Sal (Tam+Sal) or before LPS (Tam+LPS) injections normalized to control hippocampi of mice injected with

Saline (Sal). TNFα, tumor necrosis factor alpha; IL-1β, interleukin 1 beta; IL-6, interleukin 6; IL-4R, interleukin 4 receptor; TGFβ, transforming growth factor-beta. Data were obtained by 2 technical replicates; n=5-6 mice/group. Data are presented as box-and-whisker plot indicating minimum-maximum range; median and media values are shown as a horizontal line and a cross symbol. Kruskal-Wallis test followed by Dunn's post hoc test: *p< 0.05, **p<0.01. Statistical values are reported in Table S2.

Figure 3. Tamoxifen counteracts the LPS-induced dysregulation in astroglia, RGL cells and newborn neurons within the adult DG neurogenic niche. (A) Representative confocal images of double immunofluorescence for S100β (magenta) and GFAP (green) within the DG SGZ/GCL (comprised in between the dotted lines) in coronal sections. Insets show high-magnification images of GFAP+ radial glia like-cells (RGL), either S100β negative (empty white arrowheads) or S100β positive (empty pink arrowheads), and GFAP+ astrocytes (Astro) either S100β negative (full white arrowheads) or S100β positive (full pink arrowheads). (B, C) Quantification of astrocytes (B) and RGL cells (C) positive for GFAP within the DG SGZ/GCL. Densities of double-labeled GFAP+S100β+ are depicted in pink in the column graph. (D) Representative confocal images of intermediate progenitors and immature neurons positive for DCX (white) within the DG SGZ/GCL (comprised in between the dotted lines) in coronal sections. (E) Quantification of DCX+ neurogenic progenitors and immature neurons within the DG SGZ/GCL. (F) Representative confocal images of double immunofluorescence for immature neuronal marker NeuroD1 (cyan) and the proliferative marker Ki67 (red) in the DG. Full arrowheads show double NeuroD1+Ki67+ nuclei; empty arrowheads show NeuroD1+ nuclei negative for Ki67. (G, H) Quantification of double NeuroD1+Ki67+ mitotic neurogenic progenitors (G) and NeuroD1+Ki67- postmitotic immature neurons (H) within the DG GCL/SGZ (comprised in between the dotted lines); both cell populations (G, H) are negative for GFAP. Cell nuclei are counterstained with DAPI (blue, A, D, F). n=3-5 mice/group. Scale bars, 50 μm (A and D; low magnification), 25 μm (F; low magnification), and 10 μm (insets A; high magnification). Data are presented as mean ± SD. Two-way ANOVA followed by a Student-Newman-Keuls' (SNK) multiple comparison test. *p< 0.05, **p<0.01. Statistical values are reported in Tables S3a and S3b.

Figure 4. The effects of tamoxifen on the DG are long-lasting. (A) Representative confocal images depicting microglia immunopositive for Iba1 (yellow) within the DG. Insets show high-magnification images of Iba1+ microglia (arrows) for each DG sub-region (MCL, molecular cell layer; GCL, granule cell layer; Hilus). Cell nuclei are counterstained with DAPI (blue). Scale bars, 50 μm (insets scale bar, 10 μm). Quantification of Iba1+ microglial cell density (B) and area coverage (C) within DG coronal sections. Quantification of GFAP+ astrocytes (D), GFAP+ radial glial cells (RGLs) (E), neurogenic

progenitors and immature neurons positive for DCX (F) within the SGZ/GCL DG subregions. n=4-5 mice/group. Data are presented as mean ± SD. Student's t-test. *p< 0.05. Statistical values are reported in Table S4.

Figure 5. Tamoxifen counteracts LPS-induced newborn neuron and RGL cell depletion in PLX microglia-depleted mice. (A) Representative confocal images showing Iba1+ microglial cells (yellow; arrows) within the DG in coronal slices following PLX treatment (See *Fig.S4C* for the experimental design). (B-D) Quantification of Iba1+ microglia cell density within the MCL (B), GCL (C), and Hilus (D) of PLX-treated mice compared to control ones fed without PLX (dotted line). (E) Representative confocal images of neuroblasts/immature neurons positive for DCX (white) in the DG SGZ/GCL (comprised in between the dotted lines) of PLX-treated mice. (F) Quantification of DCX+ neurogenic progenitors and immature neurons within the DG SGZ/GCL. (G) Representative confocal images of double immunofluorescence for S100β (magenta) and GFAP (green) in the DG SGZ/GCL (comprised in between the dotted lines) of PLX-treated mice. Empty arrowheads indicate the radial process of GFAP+ radial glia-like cells, while full arrowheads indicate the soma of GFAP+ astrocytes. (H, I) Quantification of RGL cells (H) and astrocytes (I) positive for GFAP within the DG SGZ/GCL of the PLX-microglia depleted mice. Densities of double-labeled GFAP+S100β+ are depicted in pink in the column graph. Cell nuclei are counterstained with DAPI (blue, A,E). Scale bars, 50 μm (A, E, and G). n=4 mice/group. Data are presented as mean ± SD. Two-way ANOVA followed by a Student-Newman-Keuls' (SNK) multiple comparison test. *p< 0.05, **p<0.01. Statistical values are reported in Tables S5a and S5b.

REFERENCES

Aimone, J.B., Li, Y., Lee, S.W., Clemenson, G.D., Deng, W., and Gage, F.H. (2014). Regulation and function of adult neurogenesis: from genes to cognition. Physiol Rev *94*, 991–1026.

Arevalo, M.A., Diz-Chaves, Y., Santos-Galindo, M., Bellini, M.J., and Garcia-Segura, L.M. (2012). Selective oestrogen receptor modulators decrease the inflammatory response of glial cells. J. Neuroendocrinol. *24*, 183–190.

Arevalo, M.A., Azcoitia, I., and Garcia-Segura, L.M. (2015). The neuroprotective actions of oestradiol and oestrogen receptors. Nat. Rev. Neurosci. *16*, 17–29.

Baez-Jurado, E., Rincón-Benavides, M.A., Hidalgo-Lanussa, O., Guio-Vega, G., Ashraf, G.M., Sahebkar, A., Echeverria, V., Garcia-Segura, L.M., and Barreto, G.E. (2019). Molecular mechanisms involved in the protective actions of Selective Estrogen Receptor Modulators in brain cells. Front. Neuroendocrinol. *52*, 44–64.

Baptista, P., and Andrade, J.P. (2018). Adult hippocampal neurogenesis: Regulation and possible functional and clinical correlates. Front. Neuroanat. *12*, 44.

Batista, C.R.A., Gomes, G.F., Candelario-Jalil, E., Fiebich, B.L., and de Oliveira, A.C.P. (2019). Lipopolysaccharide-induced neuroinflammation as a bridge to understand neurodegeneration. Int. J. Mol. Sci. *20*.

Beccari, S., Valero, J., Maletic-Savatic, M., and Sierra, A. (2017). A simulation model of neuroprogenitor proliferation dynamics predicts age-related loss of hippocampal neurogenesis but not astrogenesis. Sci. Rep. *7*, 16528.

Berg, D.A., Bond, A.M., Ming, G. li, and Song, H. (2018). Radial glial cells in the adult dentate gyrus: What are they and where do they come from? F1000Research *7*.

Bonaguidi, M.A., Song, J., Ming, G.L., and Song, H. (2012). A unifying hypothesis on mammalian neural stem cell properties in the adult hippocampus. Curr. Opin. Neurobiol. *22*, 754–761.

Bonaguidi, M.M.A., Wheeler, M.M.A., Shapiro, J.J.S., Stadel, R.P., Sun, G.J., Ming, G.L., and Song, H. (2011). In vivo clonal analysis reveals self-renewing and multipotent adult neural stem cell characteristics. Cell *145*, 1142–1155.

Bond, A.M., Ming, G.L., and Song, H. (2015). Adult Mammalian Neural Stem Cells and Neurogenesis: Five Decades Later. Cell Stem Cell *17*, 385–395.

Bonzano, S., Crisci, I., Podlesny-Drabiniok, A., Rolando, C., Krezel, W., Studer, M., and De Marchis, S. (2018). Neuron-Astroglia Cell Fate Decision in the Adult Mouse Hippocampal Neurogenic Niche Is Cell-Intrinsically Controlled by COUP-TFI In Vivo. Cell Rep. *24*, 329–341.

Bonzano S, Dallorto E, Molineris I, Michelon F, Crisci I, Gambarotta G, Neri F, Oliviero S, Beckervordersandforth R, Lie DC, Peretto P, Bovetti S, Studer M, De Marchis S. (2023) NR2F1 shapes mitochondria in the mouse brain, providing new insights into Bosch-Boonstra-Schaaf optic atrophy syndrome. Dis Model Mech. 16(6):dmm049854.

Brailoiu, E., Dun, S.L., Brailoiu, G.C., Mizuo, K., Sklar, L.A., Oprea, T.I., Prossnitz, E.R., and Dun, N.J. (2007). Distribution and characterization of estrogen receptor G protein-coupled receptor 30 in the rat central nervous system. J. Endocrinol. *193*, 311–321.

Cardona, A.E., Pioro, E.P., Sasse, M.E., Kostenko, V., Cardona, S.M., Dijkstra, I.M., Huang, D.R., Kidd, G., Dombrowski, S., Dutta, R., et al. (2006). Control of microglial neurotoxicity by the fractalkine receptor. Nat. Neurosci. *9*, 917–924.

Chen, Z., Jalabi, W., Shpargel, K.B., Farabaugh, K.T., Dutta, R., Yin, X., Kidd, G.J., Bergmann, C.C., Stohlman, S.A., and Trapp, B.D. (2012). Lipopolysaccharide-induced microglial activation and neuroprotection against experimental brain injury is independent of hematogenous TLR4. J. Neurosci. *32*, 11706–11715.

Chesnokova, V., Pechnick, R.N., and Wawrowsky, K. (2016). Chronic peripheral inflammation, hippocampal neurogenesis, and behavior. Brain. Behav. Immun. *58*, 1–8.

Colón, J.M., and Miranda, J.D. (2016). Tamoxifen: An FDA approved drug with neuroprotective effects for spinal cord injury recovery. Neural Regen. Res. *11*, 1208–1211.

Correa, J., Ronchetti, S., Labombarda, F., De Nicola, A.F., and Pietranera, L. (2019). Activation of

the G Protein-Coupled Estrogen Receptor (GPER) Increases Neurogenesis and Ameliorates Neuroinflammation in the Hippocampus of Male Spontaneously Hypertensive Rats. Cell. Mol. Neurobiol.

Davis, B.M., Salinas-Navarro, M., Cordeiro, M.F., Moons, L., and Groef, L. De (2017). Characterizing microglia activation: A spatial statistics approach to maximize information extraction. Sci. Rep. *7*.

Deng, W., Aimone, J.B., and Gage, F.H. (2010). New neurons and new memories: How does adult hippocampal neurogenesis affect learning and memory? Nat. Rev. Neurosci. *11*, 339–350.

Dhaliwal, J., and Lagace, D.C. (2011). Visualization and genetic manipulation of adult neurogenesis using transgenic mice. Eur. J. Neurosci. *33*, 1025–1036.

Diaz-Aparicio, I., Paris, I., Sierra-Torre, V., Plaza-Zabala, A., Rodríguez-Iglesias, N., Márquez-Ropero, M., Beccari, S., Huguet, P., Abiega, O., Alberdi, E., et al. (2020). Microglia Actively Remodel Adult Hippocampal Neurogenesis through the Phagocytosis Secretome. J. Neurosci. *40*, 1453–1482.

DonCarlos, L.L., Azcoitia, I., and Garcia-Segura, L.M. (2009). Neuroprotective actions of selective estrogen receptor modulators. Psychoneuroendocrinology *34*.

Dranovsky, A., Picchini, A.M., Moadel, T., Sisti, A.C., Yamada, A., Kimura, S., Leonardo, E.D., and Hen, R. (2011). Experience Dictates Stem Cell Fate in the Adult Hippocampus. Neuron *70*, 908–923.

Dumas, A. A., Borst, K., & Prinz, M. (2021). Current tools to interrogate microglial biology. Neuron, 109(18), 2805-2819.

Ekdahl, C.T. (2012). Microglial activation-tuning and pruning adult neurogenesis. Front. Pharmacol. *3 MAR*, 41.

Ekdahl, C.T., Claasen, J.H., Bonde, S., Kokaia, Z., and Lindvall, O. (2003). Inflammation is detrimental for neurogenesis in adult brain. Proc. Natl. Acad. Sci. U. S. A. *100*, 13632–13637.

Elmore, M.R.P., Najafi, A.R., Koike, M.A., Dagher, N.N., Spangenberg, E.E., Rice, R.A., Kitazawa, M., Matusow, B., Nguyen, H., West, B.L., et al. (2014). Colony-stimulating factor 1 receptor signaling is necessary for microglia viability, unmasking a microglia progenitor cell in the adult brain. Neuron *82*, 380–397.

Encinas, J.M., Michurina, T. V., Peunova, N., Park, J.H., Tordo, J., Peterson, D.A., Fishell, G., Koulakov, A., and Enikolopov, G. (2011). Division-coupled astrocytic differentiation and age-related depletion of neural stem cells in the adult hippocampus. Cell Stem Cell *8*, 566–579.

Farrar MC, Jacobs TF. Tamoxifen. 2023 Apr 10. In: StatPearls [Internet]. Treasure Island (FL): StatPearls Publishing; 2023 Jan–. PMID: 30422500.

Fernández-Arjona, M. del M., Grondona, J.M., Granados-Durán, P., Fernández-Llebrez, P., and López-Ávalos, M.D. (2017). Microglia morphological categorization in a rat model of neuroinflammation by hierarchical cluster and principal components analysis. Front. Cell. Neurosci. *11*, 1–22.

Frost, J.L., and Schafer, D.P. (2016). Microglia: Architects of the Developing Nervous System. Trends Cell Biol. *26*, 587–597.

Fujioka, H., and Akema, T. (2010). Lipopolysaccharide acutely inhibits proliferation of neural precursor cells in the dentate gyrus in adult rats. Brain Res. *1352*, 35–42.

Gao, Z., Ure, K., Ables, J.L., Lagace, D.C., Nave, K.A., Goebbels, S., Eisch, A.J., and Hsieh, J. (2009). Neurod1 is essential for the survival and maturation of adult-born neurons. Nat. Neurosci. *12*, 1090–1092.

Garcia-Ovejero, D., Azcoitia, I., DonCarlos, L.L., Melcangi, R.C., and Garcia-Segura, L.M. (2005). Glia-neuron crosstalk in the neuroprotective mechanisms of sex steroid hormones. Brain Res. Rev. *48*, 273–286.

Gebara, E., Sultan, S., Kocher-Braissant, J., and Toni, N. (2013). Adult hippocampal neurogenesis inversely correlates with microglia in conditions of voluntary running and aging. Front. Neurosci. *7*, 145.

Gebara, E., Bonaguidi, M.A., Beckervordersandforth, R., Sultan, S., Udry, F., Gijs, P.J., Lie, D.C., Ming, G.L., Song, H., and Toni, N. (2016). Heterogeneity of Radial Glia-Like Cells in the Adult Hippocampus. Stem Cells *34*, 997–1010.

Gonçalves, J.T., Schafer, S.T., and Gage, F.H. (2016). Adult Neurogenesis in the Hippocampus: From Stem Cells to Behavior. Cell *167*, 897–914.

Green, K.N., Crapser, J.D., and Hohsfield, L.A. (2020). To Kill a Microglia: A Case for CSF1R Inhibitors. Trends Immunol. *41*, 771–784.

Hajszan, T., Milner, T.A., and Leranth, C. (2007). Sex steroids and the dentate gyrus. Prog. Brain Res. *163*, 399–416.

Harris, L., Rigo, P., Stiehl, T., Gaber, Z.B., Austin, S.H.L., Masdeu, M. del M., Edwards, A., Urbán, N., Marciniak-Czochra, A., and Guillemot, F. (2021). Coordinated changes in cellular behavior ensure the lifelong maintenance of the hippocampal stem cell population. Cell Stem Cell 1–14.

Hayashi, S., and McMahon, A.P. (2002). Efficient recombination in diverse tissues by a tamoxifen-inducible form of Cre: A tool for temporally regulated gene activation/inactivation in the mouse. Dev. Biol. *244*, 305–318.

Hirrlinger, P.G., Scheller, A., Braun, C., Hirrlinger, J., and Kirchhoff, F. (2006). Temporal control of gene recombination in astrocytes by transgenic expression of the tamoxifen-inducible DNA recombinase variant CreERT2. Glia *54*, 11–20.

Huang, Y., Xu, Z., Xiong, S., Sun, F., Qin, G., Hu, G., Wang, J., Zhao, L., Liang, Y.X., Wu, T., et al. (2018). Repopulated microglia are solely derived from the proliferation of residual microglia after acute depletion. Nat. Neurosci. *21*, 530–540.

Ibrayeva, A., Bay, M., Pu, E., Jörg, D.J., Peng, L., Jun, H., Zhang, N., Aaron, D., Lin, C., Resler, G., et al. (2021). Early stem cell aging in the mature brain. Cell Stem Cell *28*, 955-966.e7.

Imayoshi, I., Sakamoto, M., and Kageyama, R. (2011). Genetic methods to identify and manipulate newly born neurons in the adult brain. Front. Neurosci. *5*, 1–11.

Isgor, C., and Watson, S.J. (2005). Estrogen receptor α and β mRNA expressions by proliferating and differentiating cells in the adult rat dentate gyrus and subventricular zone. Neuroscience *134*, 847–856.

Ito, D., Imai, Y., Ohsawa, K., Nakajima, K., Fukuuchi, Y., and Kohsaka, S. (1998). Microglia-specific localisation of a novel calcium binding protein, Iba1. Mol. Brain Res. *57*, 1–9.

Jahn, H.M., Kasakow, C. V., Helfer, A., Michely, J., Verkhratsky, A., Maurer, H.H., Scheller, A., and Kirchhoff, F. (2018). Refined protocols of tamoxifen injection for inducible DNA recombination in mouse astroglia. Sci. Rep. *8*, 5913.

Jordan, V.C. (2003). Tamoxifen: A most unlikely pioneering medicine. Nat. Rev. Drug Discov. *2*, 205–213.

Jung H, Lee D, You H, Lee M, Kim H, Cheong E, Um JW. (2023). LPS induces microglial activation and GABAergic synaptic deficits in the hippocampus accompanied by prolonged cognitive impairment. Sci Rep. 13(1):6547.

Kee, N., Sivalingam, S., Boonstra, R., and Wojtowicz, J.M. (2002). The utility of Ki-67 and BrdU as proliferative markers of adult neurogenesis. J. Neurosci. Methods *115*, 97–105.

Kempermann, G., Song, H., and Gage, F.H. (2015). Neurogenesis in the adult hippocampus. Cold Spring Harb. Perspect. Biol. *7*.

Kohman, R.A., and Rhodes, J.S. (2013). Neurogenesis, inflammation and behavior. Brain. Behav. Immun. *27*, 22–32.

Lana, D., Ugolini, F., Nosi, D., Wenk, G.L., and Giovannini, M.G. (2017). Alterations in the interplay between neurons, astrocytes and microglia in the rat dentate gyrus in experimental models of neurodegeneration. Front. Aging Neurosci. *9*, 1–17.

Lee, C.-M.M., Zhou, L., Liu, J., Shi, J., Geng, Y., Wang, J.J., Su, X., Barad, N., Wang, J.J., Sun, Y.E., et al. (2020). Single-cell RNA-seq analysis revealed long-lasting adverse effects of tamoxifen on neurogenesis in prenatal and adult brains. Proc. Natl. Acad. Sci. U. S. A. *117*, 19578–19589.

Leiter, O., Kempermann, G., and Walker, T.L. (2016). A Common Language: How neuroimmunological cross talk regulates adult hippocampal neurogenesis. Stem Cells Int. *2016*.

Lien, E.A., Wester, K., Lonning, P.E., Solheim, E., and Ueland, P.M. (1991). Distribution of tamoxifen and metabolites into brain tissue and brain metastases in breast cancer patients. Br. J. Cancer *63*, 641–645.

Madore, C., Joffre, C., Delpech, J.C., De Smedt-Peyrusse, V., Aubert, A., Coste, L., Layé, S., and Nadjar, A. (2013). Early morphofunctional plasticity of microglia in response to acute lipopolysaccharide. Brain. Behav. Immun. *34*, 151–158.

Martinkovich S, Shah D, Planey SL, Arnott JA. Selective estrogen receptor modulators: tissue specificity and clinical utility (2014). Clin Interv Aging. 28;9:1437-52.

Mazzucco, C.A., Lieblich, S.E., Bingham, B.I., Williamson, M.A., Viau, V., and Galea, L.A.M. (2006). Both estrogen receptor α and estrogen receptor β agonists enhance cell proliferation in the dentate gyrus of adult female rats. Neuroscience *141*, 1793–1800.

Melo-Salas, M.S., Pérez-Domínguez, M., and Zepeda, A. (2018). Systemic Inflammation Impairs Proliferation of Hippocampal Type 2 Intermediate Precursor Cells. Cell. Mol. Neurobiol. *38*, 1517–1528.

Monje, M.L., Toda, H., and Palmer, T.D. (2003). Inflammatory blockade restores adult hippocampal neurogenesis. Science *302*, 1760–1765.

Morganti, J.M., Riparip, L.K., and Rosi, S. (2016). Call off the dog(ma): M1/M2 polarization is concurrent following traumatic brain injury. PLoS One *11*, 1–13.

Mori, T., Tanaka, K., Buffo, A., Wurst, W., Kühn, R., and Gotz, M. (2006). Inducible gene deletion in astroglia and radial glia - A valuable tool for functional and lineage analysis. Glia *54*, 21–34.

Nato G, Caramello A, Trova S, Avataneo V, Rolando C, Taylor V, Buffo A, Peretto P, Luzzati F. (2015). Striatal astrocytes produce neuroblasts in an excitotoxic model of Huntington's disease. Development. 142(5):840-5.

Norden, D.M., Trojanowski, P.J., Villanueva, E., Navarro, E., and Godbout, J.P. (2016). Sequential activation of microglia and astrocyte cytokine expression precedes increased iba-1 or GFAP immunoreactivity following systemic immune challenge. Glia 64, 300–316.

Oboti L, Trova S, Schellino R, Marraudino M, Harris NR, Abiona OM, Stampar M, Lin W, Peretto P. (2017) Activity Dependent Modulation of Granule Cell Survival in the Accessory Olfactory Bulb at Puberty. Front Neuroanat. 11:44. doi: 10.3389/fnana.2017.00044.

Pareto, D., Alvarado, M., Hanrahan, S.M., and Biegon, A. (2004). In vivo occupancy of female rat brain estrogen receptors by 17β-estradiol and tamoxifen. Neuroimage *23*, 1161–1167.

Perez-Dominguez, M., Ávila-Muñoz, E., Domínguez-Rivas, E., and Zepeda, A. (2019). The detrimental effects of lipopolysaccharide-induced neuroinflammation on adult hippocampal neurogenesis depend on the duration of the pro-inflammatory response. Neural Regen. Res. *14*, 817–825.

Pérez-Domínguez, M., Tovar-Y-Romo, L.B., and Zepeda, A. (2017). Neuroinflammation and physical exercise as modulators of adult hippocampal neural precursor cell behavior. Rev. Neurosci. *29*, 1–20.

Perry, V.H., Nicoll, J.A.R., and Holmes, C. (2010). Microglia in neurodegenerative disease. Nat. Rev. Neurol. *6*, 193–201.

Procaccini, C., De Rosa, V., Pucino, V., Formisano, L., and Matarese, G. (2015). Animal models of Multiple Sclerosis. Eur. J. Pharmacol. *759*, 182–191.

Raj, D.D.D.A., Jaarsma, D., Holtman, I.R., Olah, M., Ferreira, F.M., Schaafsma, W., Brouwer, N., Meijer, M.M., de Waard, M.C., van der Pluijm, I., et al. (2014). Priming of microglia in a DNA-repair deficient model of accelerated aging. Neurobiol. Aging *35*, 2147–2160.

Rolando, C., Parolisi, R., Boda, E., Schwab, M.E., Rossi, F., and Buffo, A. (2012). Distinct roles of Nogo-A and nogo receptor 1 in the homeostatic regulation of adult neural stem cell function and neuroblast migration. J. Neurosci. *32*, 17788–17799.

Rotheneichner, P., Romanelli, P., Bieler, L., Pagitsch, S., Zaunmair, P., Kreutzer, C., König, R., Marschallinger, J., Aigner, L., and Couillard-Després, S. (2017). Tamoxifen activation of cre-recombinase has no persisting effects on adult neurogenesis or learning and anxiety. Front. Neurosci. *11*, 1–8.

Sahay, A., Scobie, K.N., Hill, A.S., O'Carroll, C.M., Kheirbek, M.A., Burghardt, N.S., Fenton, A.A.,

Dranovsky, A., and Hen, R. (2011). Increasing adult hippocampal neurogenesis is sufficient to improve pattern separation. Nature *472*, 466–470.

Schneider CA, Rasband WS, Eliceiri KW. NIH Image to ImageJ: 25 years of image analysis. Nat Methods. 2012 Jul;9(7):671-5. doi: 10.1038/nmeth.2089. PMID: 22930834; PMCID: PMC5554542.

Semerci, F., and Maletic-Savatic, M. (2016). Transgenic mouse models for studying adult neurogenesis. Front. Biol. (Beijing). *11*, 151–167.

Sisk CL, Zehr JL. (2005). Pubertal hormones organize the adolescent brain and behavior. Front Neuroendocrinol. 26(3-4):163-74.

Sierra, A., Gottfried-Blackmore, A., Milner, T.A., McEwen, B.S., and Bulloch, K. (2008). Steroid hormone receptor expression and function in microglia. Glia *56*, 659–674.

Sierra, A., Encinas, J.M., Deudero, J.J.P., Chancey, J.H., Enikolopov, G., Overstreet-Wadiche, L.S., Tsirka, S.E., and Maletic-Savatic, M. (2010). Microglia shape adult hippocampal neurogenesis through apoptosis-coupled phagocytosis. Cell Stem Cell *7*, 483–495.

Sierra, A., Beccari, S., Diaz-Aparicio, I., Encinas, J.M., Comeau, S., and Tremblay, M.È. (2014). Surveillance, phagocytosis, and inflammation: How never-resting microglia influence adult hippocampal neurogenesis. Neural Plast. *2014*.

Sierra, A., Martín-Suárez, S., Valcárcel-Martín, R., Pascual-Brazo, J., Aelvoet, S.A., Abiega, O., Deudero, J.J., Brewster, A.L., Bernales, I., Anderson, A.E., et al. (2015). Neuronal hyperactivity accelerates depletion of neural stem cells and impairs hippocampal neurogenesis. Cell Stem Cell *16*, 488–503.

Smith BM, Saulsbery AI, Sarchet P, Devasthali N, Einstein D, Kirby ED. (2022) Oral and Injected Tamoxifen Alter Adult Hippocampal Neurogenesis in Female and Male Mice. eNeuro. 0422-21.2022.

Snyder, J.S., Soumier, A., Brewer, M., Pickel, J., and Cameron, H.A. (2011). Adult hippocampal neurogenesis buffers stress responses and depressive behaviour. Nature *476*, 458–462.

Song, J., Zhong, C., Bonaguidi, M.A., Sun, G.J., Hsu, D., Gu, Y., Meletis, K., Huang, Z.J., Ge, S., Enikolopov, G., et al. (2012). Neuronal circuitry mechanism regulating adult quiescent neural stem-cell fate decision. Nature *489*, 150–154.

Steiner, B., Kronenberg, G., Jessberger, S., Brandt, M.D., Reuter, K., and Kempermann, G. (2004). Differential regulation of gliogenesis in the context of adult hippocampal neurogenesis in mice. Glia *46*, 41–52.

Steiner, B., Klempin, F., Wang, L., Kott, M., Kettenmann, H., and Kempermann, G. (2006). Type-2 cells as link between glial and neuronal lineage in adult hippocampal neurogenesis. Glia *54*, 805–814.

Steiner, B., Zurborg, S., Hörster, H., Fabel, K., and Kempermann, G. (2008). Differential 24 h responsiveness of Prox1-expressing precursor cells in adult hippocampal neurogenesis to physical activity, environmental enrichment, and kainic acid-induced seizures. Neuroscience *154*, 521–529.

Stence, N., Waite, M., and Dailey, M.E. (2001). Dynamics of microglial activation: A confocal time-lapse analysis in hippocampal slices. Glia *33*, 256–266.

Sun, X., Ji, C., Hu, T., Wang, Z., and Chen, G. (2013). Tamoxifen as an effective neuroprotectant

against early brain injury and learning deficits induced by subarachnoid hemorrhage: Possible involvement of inflammatory signaling. J. Neuroinflammation *10*, 157.

Tapia-Gonzalez, S., Carrero, P., Pernia, O., Garcia-Segura, L.M., and Diz-Chaves, Y. (2008). Selective oestrogen receptor (ER) modulators reduce microglia reactivity in vivo after peripheral inflammation: potential role of microglial ERs. J. Endocrinol. *198*, 219–230.

Tian, D.S., Liu, J.L., Xie, M.J., Zhan, Y., Qu, W.S., Yu, Z.Y., Tang, Z.P., Pan, D.J., and Wang, W. (2009). Tamoxifen attenuates inflammatory-mediated damage and improves functional outcome after spinal cord injury in rats. J. Neurochem. *109*, 1658–1667.

Toda, T., Parylak, S.L., Linker, S.B., and Gage, F.H. (2019). The role of adult hippocampal neurogenesis in brain health and disease. Mol. Psychiatry 24, 67–87.

Trova S, Bovetti S, Pellegrino G, Bonzano S, Giacobini P, Peretto P. (2020) HPG-Dependent Peri-Pubertal Regulation of Adult Neurogenesis in Mice. Front Neuroanat. 14:584493.

Trova S, Bovetti S, Bonzano S, De Marchis S, Peretto P. (2021) Sex Steroids and the Shaping of the Peripubertal Brain: The Sexual-Dimorphic Set-Up of Adult Neurogenesis. Int J Mol Sci. 22(15):7984.

Valero, J., Mastrella, G., Neiva, I., Sánchez, S., and Malva, J.O. (2014). Long-term effects of an acute and systemic administration of LPS on adult neurogenesis and spatial memory. Front. Neurosci. *8*, 1–13.

Valny, M., Honsa, P., Kirdajova, D., Kamenik, Z., and Anderova, M. (2016). Tamoxifen in the mouse brain: Implications for fate-mapping studies using the tamoxifen-inducible cre-loxP system. Front. Cell. Neurosci. *10*, 243.

Vicidomini, C., Guo, N., and Sahay, A. (2020). Communication, Cross Talk, and Signal Integration in the Adult Hippocampal Neurogenic Niche. Neuron *105*, 220–235.

Walker, F.R., Beynon, S.B., Jones, K.A., Zhao, Z., Kongsui, R., Cairns, M., and Nilsson, M. (2014). Dynamic structural remodelling of microglia in health and disease: A review of the models, the signals and the mechanisms. Brain. Behav. Immun. *37*, 1–14.

Wang, X., Zhao, L., Zhang, Y., Ma, W., Gonzalez, S.R., Fan, J., Kretschmer, F., Badea, T.C., Qian, H.H., and Wong, W.T. (2017). Tamoxifen provides structural and functional rescue in murine models of photoreceptor degeneration. J. Neurosci. *37*, 3294–3310.

Wendeln A.C., Degenhardt K., Kaurani L., Gertig M., Ulas T., Jain G., Wagner J., Häsler L.M., Wild K., Skodras A., Blank T., Staszewski O., Datta M., Centeno T.P., Capece V., Islam M.R., Kerimoglu C., Staufenbiel M., Schultze J.L., Beyer M., Prinz M., Jucker M., Fischer A., Neher J.J. Innate immune memory in the brain shapes neurological disease hallmarks. Nature. 2018 556(7701):332-338.

Whitfield J, Littlewood T, Soucek L. (2015). Tamoxifen administration to mice. Cold Spring Harb Protoc. (3):269-71. Woodbury, M.E., Freilich, R.W., Cheng, C.J., Asai, H., Ikezu, S., Boucher, J.D., Slack, F., and Ikezu, T. (2015). miR-155 is essential for inflammation-induced hippocampal neurogenic dysfunction. J. Neurosci. *35*, 9764–9781.

Wu, M.D., Hein, A.M., Moravan, M.J., Shaftel, S.S., Olschowka, J.A., O'Banion, M.K., and Kerry O 'banion, M. (2012). Adult murine hippocampal neurogenesis is inhibited by sustained IL-1β and not rescued by voluntary running. Brain. Behav. Immun. *26*, 292–300.

Yang, Q. qiao, and Zhou, J. wei (2019). Neuroinflammation in the central nervous system: Symphony of glial cells. Glia *67*, 1017–1035.

Yang, S.M., Alvarez, D.D., and Schinder, A.F. (2015). Reliable genetic labeling of adult-born dentate granule cells using ascl1CreERT2 and glastCreERT2 murine lines. J. Neurosci. *35*, 15379–15390.

Zhang, J., Giesert, F., Kloos, K., Vogt Weisenhorn, D.M., Aigner, L., Wurst, W., and Couillard-Despres, S. (2010). A powerful transgenic tool for fate mapping and functional analysis of newly generated neurons. BMC Neurosci. *11*.

Zhang, J., He, H., Qiao, Y., Zhou, T., He, H., Yi, S., Zhang, L., Mo, L., Li, Y., Jiang, W., et al. (2020). Priming of microglia with IFN-γ impairs adult hippocampal neurogenesis and leads to depression-like behaviors and cognitive defects. Glia 1–19.

Zhao, L., O'Neill, K., and Diaz Brinton, R. (2005). Selective estrogen receptor modulators (SERMs) for the brain: Current status and remaining challenges for developing NeuroSERMs. Brain Res. Rev. *49*, 472–493.

Zonis, S., Ljubimov, V.A., Mahgerefteh, M., Pechnick, R.N., Wawrowsky, K., and Chesnokova, V. (2013). p21Cip restrains hippocampal neurogenesis and protects neuronal progenitors from apoptosis during acute systemic inflammation. Hippocampus *23*, 1383–1394.

FIGURES

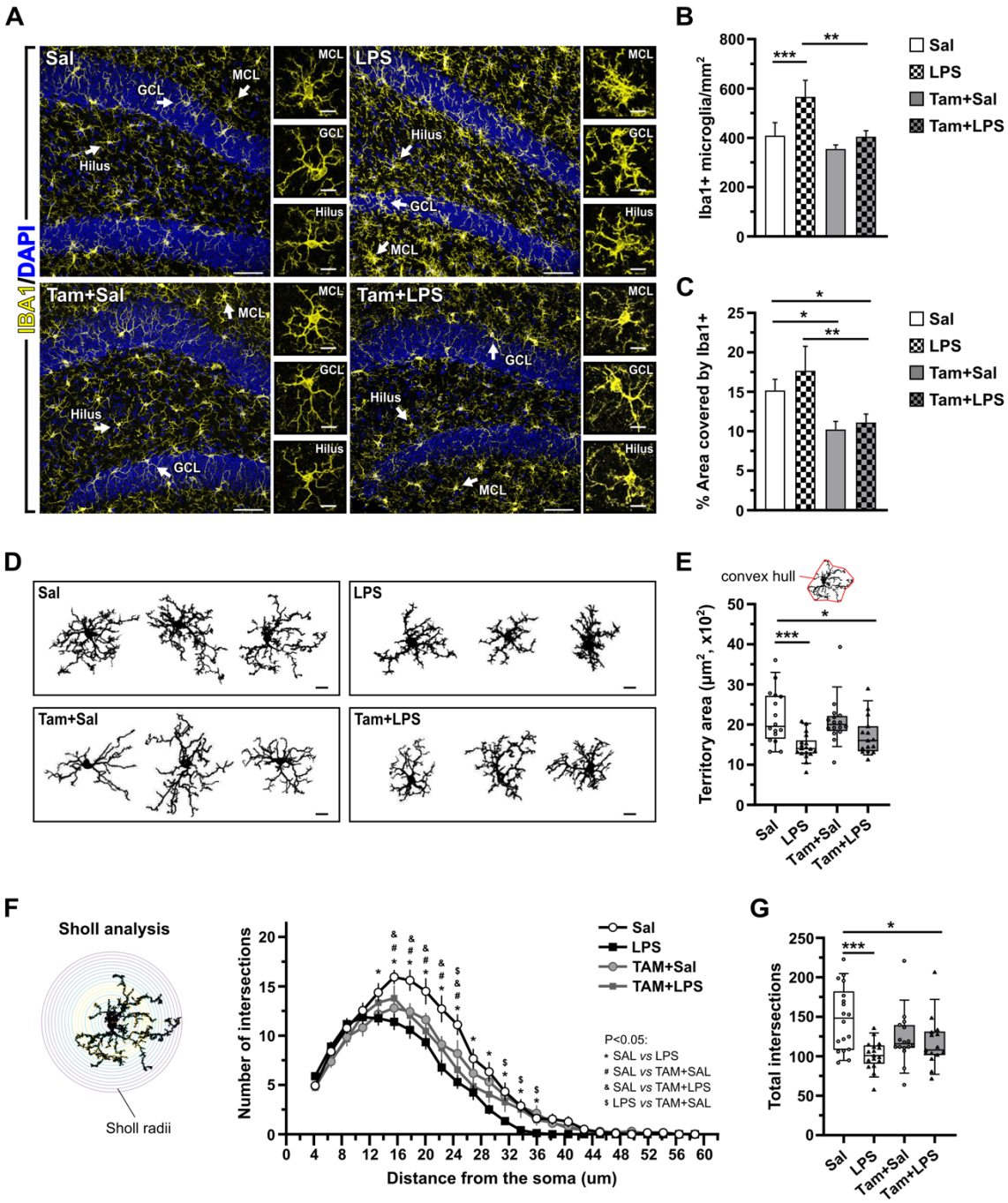
A
Sal
LPS
Tam+Sal
Tam+LPS
IBA1/DAPI
MCL
GCL
Hilus
B
Iba1+ microglia/mm2
Sal
LPS
Tam+Sal
Tam+LPS
C
% Area covered by Iba1+
D
E
convex hull
Territory area (µm2, x102)
F
Sholl analysis
Sholl radii
Number of intersections
Distance from the soma (um)
P<0.05:
* SAL vs LPS
# SAL vs TAM+SAL
& SAL vs TAM+LPS
$ LPS vs TAM+SAL
G
Total intersections

Figure 1

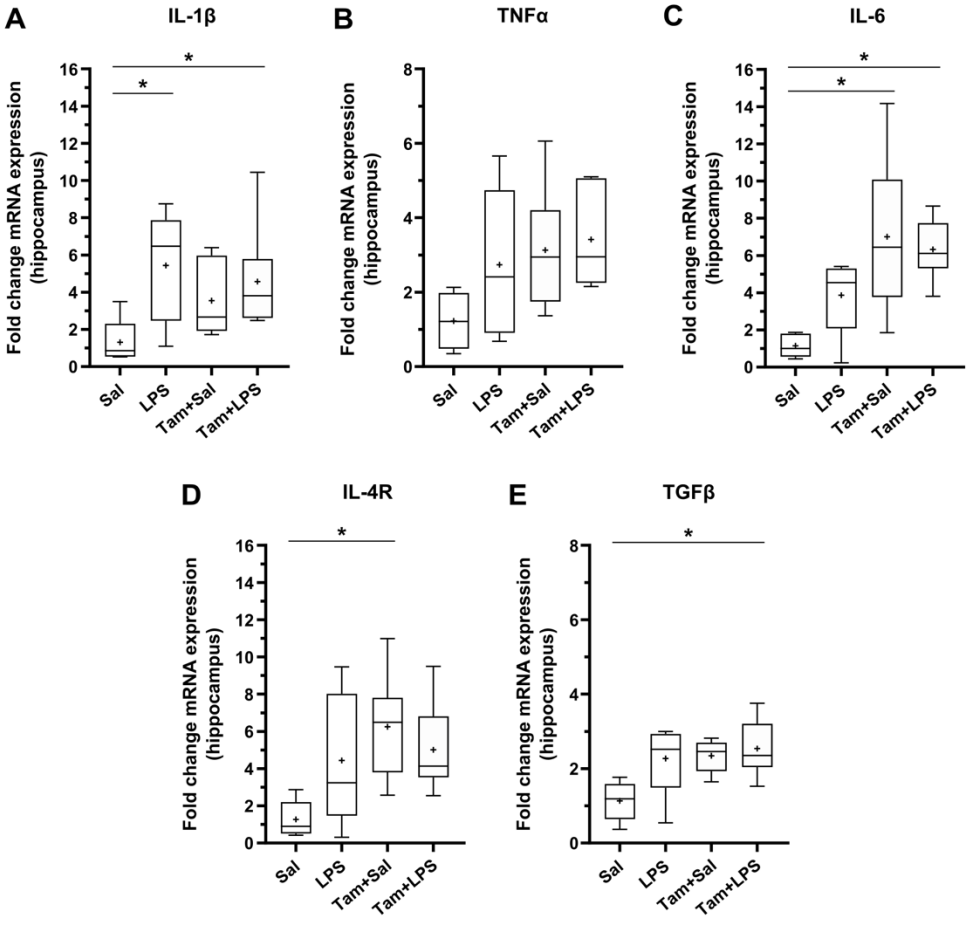
A
IL-1β
B
TNFα
C
IL-6
D
IL-4R
E
TGFβ
Fold change mRNA expression (hippocampus)
Sal
LPS
Tam+Sal
Tam+LPS
*

Figure 2

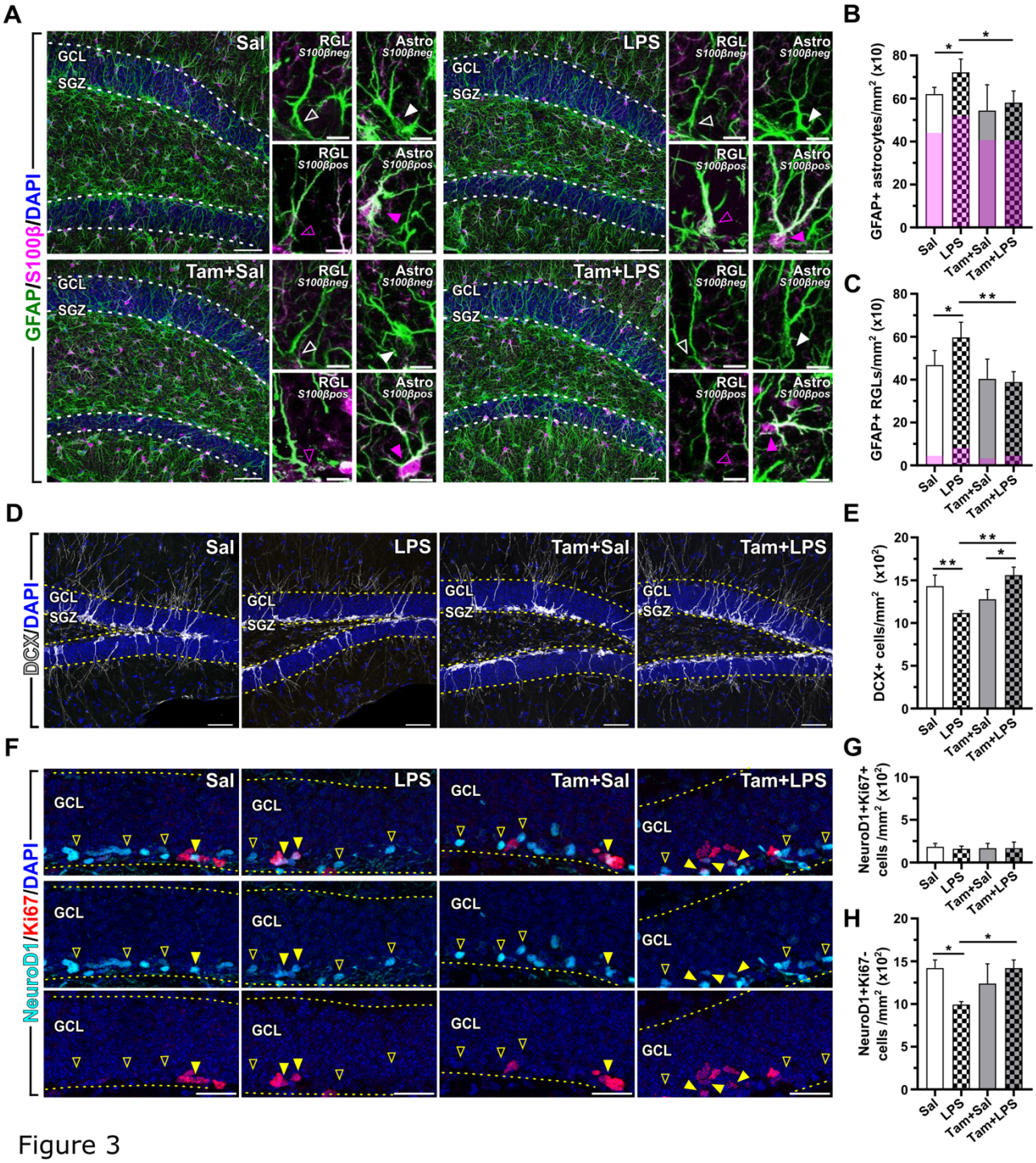
A
Sal
LPS
Tam+Sal
Tam+LPS
GCL
SGZ
RGL S100βneg
Astro S100βneg
RGL S100βpos
Astro S100βpos
GFAP/S100β/DAPI
B
GFAP+ astrocytes/mm² (x10)
C
GFAP+ RGLs/mm² (x10)
D
DCX/DAPI
E
DCX+ cells/mm² (x10²)
F
NeuroD1/Ki67/DAPI
G
NeuroD1+Ki67+ cells /mm² (x10²)
H
NeuroD1+Ki67- cells /mm² (x10²)

Figure 3

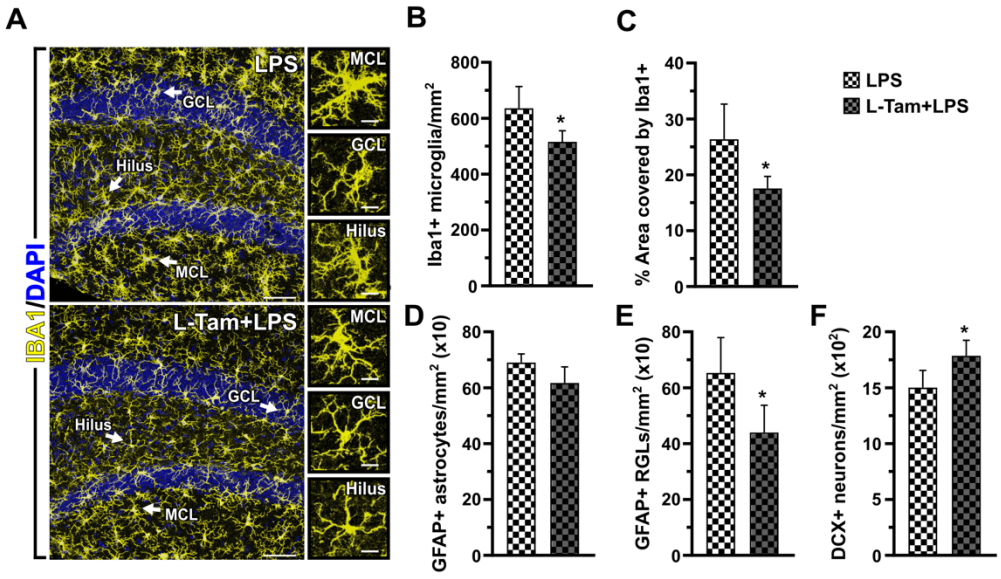
A
LPS
GCL
Hilus
MCL
L-Tam+LPS
IBA1/DAPI
B
Iba1+ microglia/mm2
C
% Area covered by Iba1+
LPS
L-Tam+LPS
D
GFAP+ astrocytes/mm2 (x10)
E
GFAP+ RGLs/mm2 (x10)
F
DCX+ neurons/mm2 (x102)

Figure 4

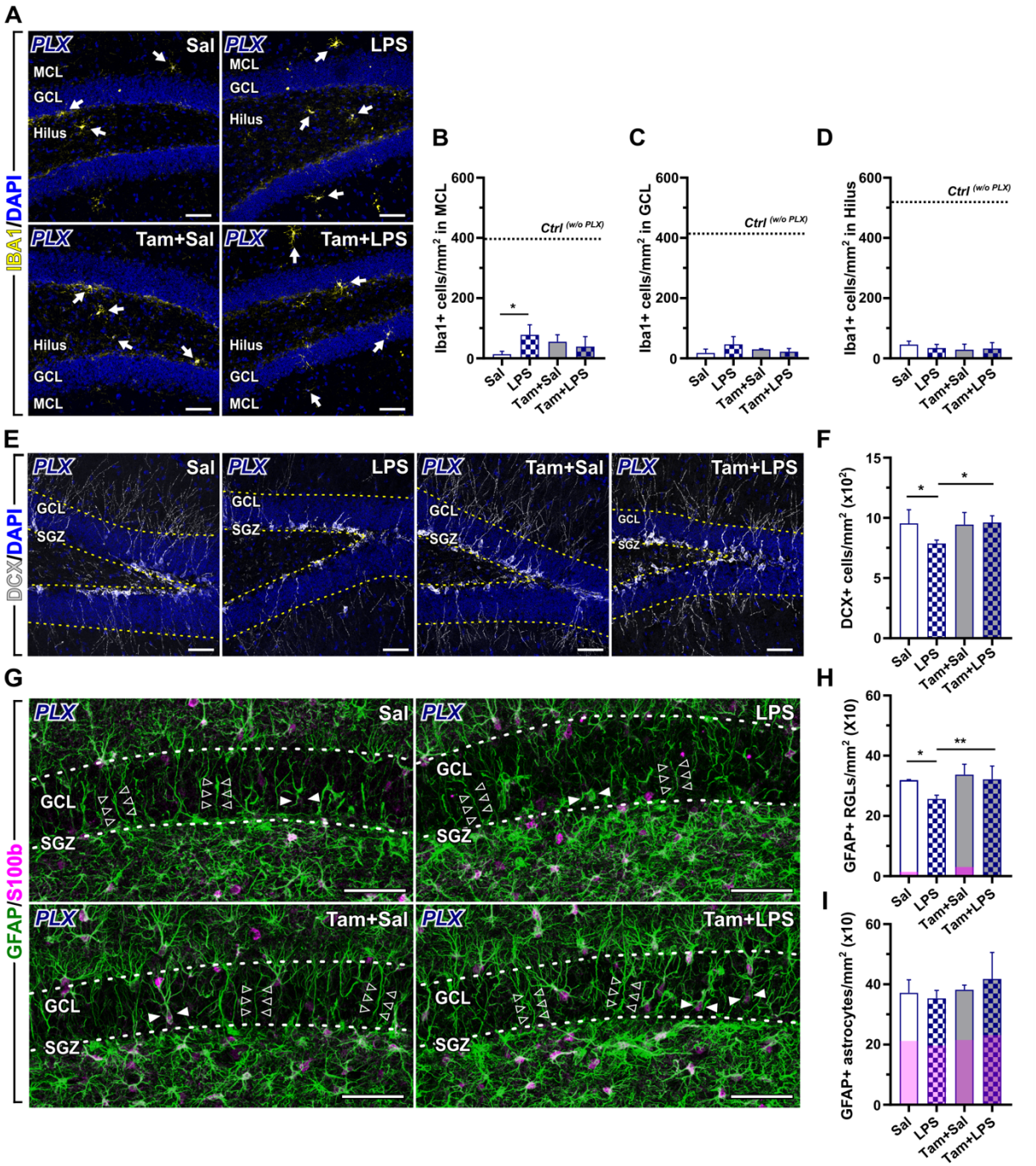
A
PLX
Sal
LPS
Tam+Sal
Tam+LPS
MCL
GCL
Hilus
IBA1/DAPI
B
C
D
Iba1+ cells/mm2 in MCL
Iba1+ cells/mm2 in GCL
Iba1+ cells/mm2 in Hilus
Ctrl (w/o PLX)
600
400
200
0
*
Sal
LPS
Tam+Sal
Tam+LPS
E
SGZ
DCX/DAPI
F
DCX+ cells/mm2 (x10²)
15
10
5
G
GFAP/S100b
H
GFAP+ RGLs/mm2 (X10)
60
40
20
**
I
GFAP+ astrocytes/mm2 (x10)

Figure 5